A Neural Network-Based Controller Towards Achieving Near-Natural Gait in Transfemoral Amputees

Zunaed Kibria[*] and Sesh Commuri[†]

Electrical and Biomedical Department, University of Nevada - Reno, Reno, Nevada, U.S.A.

Keywords: Prosthetic Control, Radial Basis Function Based Neural Network (RBFNN), Gait Analysis.

Abstract: Achieving proper post-amputation mobility in an individual is extremely important to ensure the health of the residual limb and the quality of life of an individual. Traditionally, prosthetic limbs were designed to primarily support the weight of the individual and replicate the look and feel of the natural limb. Powered prosthetic devices are typically based on classical control and cannot adapt to changing user requirements. A critical challenge in controller design is that, unlike tracking controllers, the desired trajectory for the prosthetic joint is unknown. Improper control can lead to asymmetry in the gait of intact and amputated sides, which in turn can have adverse health consequences. In this paper, an intelligent controller for above-knee prosthesis is proposed that can generate pseudo-trajectories for the joints, learn the dynamics of the prosthetic limb in real-time, and track these pseudo-trajectories to reduce the asymmetry in gait between the intact and amputated side. Mathematical analysis shows that the method is stable and can adapt to changing user gaits. Numerical simulations and Monte Carlo analysis show that the performance of the controller is robust to variations in dynamics and user requirements, and results in near-natural gait for the individual.

1 INTRODUCTION

Amputation of the lower limb is performed as a consequence of traumatic injuries or diseases such as diabetes and vascular disorders (Gorden et al., 2022). After amputation, the residual limb is fitted with a socket, and a prosthetic limb is attached to the socket. Traditionally, such prosthetic limbs are designed to provide weight bearing and limited mobility. Modern powered devices can help in locomotion by providing regenerative energy as well as providing custom fit for the individual. However, an individual seldom regains natural locomotion as these devices cannot recognize and adapt to changing user gait or environmental conditions.

Effective control mechanisms are essential for improving prosthetic gait. Passive devices, acting as springs or dampers, provide weight support but limit mobility and increase energy expenditure during locomotion (Feng & Wang, 2017; Sharma et al., 2022). Semi-active and active prostheses offer some improvement, but they cannot adjust to different gait patterns (Saini et al., 2020) and rely on traditional

control methods which cannot compensate for system nonlinearities (Elery et al., 2020; Lenzi et al., 2019). Researchers also explored several adaptive control methods (Embry & Gregg, 2021; Gao et al., 2021). Model reference adaptive control performs best among them but is based on a linearized model with limited range of performance and does not provide a symmetric gait (Pagel et al., 2017) .

In this paper, a neural network-based control strategy is pursued to reduce the asymmetry in gait between the intact and amputated side of an amputee. Gait is primarily divided into two phases: stance and swing. The stance phase is further subdivided into phases including Heel Strike, Loading Response, Mid Stance, Terminal Stance, and Pre-Swing, while the swing phase comprises Toe Off, Mid Swing, and Terminal Swing. During gait, the body weight is supported by a single leg from 'Loading Response' to 'Terminal Stance' phases, and the time difference between these phases is defined as 'single support time'. When the difference in single support time between the intact and prosthetic side is minimized, it promotes smoother weight transfer between the legs,

---

[*] https://www.linkedin.com/in/zunaed-kibria-984743107/

[†] https://www.unr.edu/ebme/people/sesh-commuri

reduces gait asymmetry, aids amputees in achieving a more natural and balanced gait.

The following approach is adopted to implement a learning controller that can adapt to user requirements and guarantee near natural gait in an individual:

- Develop the dynamical model of the prosthetic leg system to determine the nature of unknown nonlinear functions that influence the dynamics.

- Desired trajectories for the knee and ankle joints are first selected based on the natural displacement profile of these joints in an intact individual and then parameterize in terms of the gait speed.

- Use a visco-elastic model to estimate ground reaction force and reaction torques at the joints, and then compensate for them in the system dynamics.

- A radial basis function based neural network (RBFNN) is selected to learn the unknown nonlinear parameters in the dynamics due to its efficiency and lower computational cost (Schilling et al., 2001).

- Cost function reflecting the asymmetry between the gait of the intact and prosthetic side is used to perform Lyapunov analysis. Weight update laws for the neural network are determined so that the unknown/changing dynamics are estimated while ensuring stability of the controlled system and minimizing the cost, i.e., the asymmetry in the gait.

Numerical simulations are used to demonstrate the ability of the control strategy to accommodate variations in height, weight, gait speed, and ground reaction force. Analysis shows that the time duration of the single support portion of the gait is improved with the proposed control strategy, thereby minimizing the asymmetry in the gait.

The rest of the paper is organized as follows – in section 2, gait requirements for transfemoral prosthesis, detailed formulation for control mechanism, and stability of the closed loop system are presented. Numerical simulations and Monte Carlo analysis to evaluate the ability of the proposed control scheme are demonstrated in section 3. The conclusions of the paper and future work are presented in section 4.

2 CONTROL OF THE PROSTHESIS JOINT

2.1 Gait Requirement for Transfemoral Prosthesis

The nominal displacement profiles for the knee and ankle joints in a healthy individual during normal gait is shown in Figure 1(a). It is desirable for the prosthetic limb to track similar displacement profile in order to achieve near normal gait. Similar to the technique followed in (Winter, 2009), we can calculate the joint angles of lower limb as shown in Figure 1(b). Assuming that the user is walking with upright posture ($q\_tr = 90°$) and the joints follow the nominal displacement profiles mentioned in Figure 1(a), we can calculate the ideal foot position relative to the ground during gait (Figure 1(c)). Postural balance relies on smooth weight transfer between the legs. If a prosthetic device effectively tracks the movements of the knee, ankle, and foot to closely replicate those on the intact side, it would lead to improved weight transfer and reduce gait asymmetry. (It is to be noted that the analysis is limited to motion in the sagittal plane.)

2.2 System Model

The dynamics of knee-ankle prosthetic system (Figure 1(d)) can be expressed as:

$$M_{ka}(q)\ddot{q} + V_{ka}(q,\dot{q})\dot{q} + G_{ka}(q) + F_{ka}(\dot{q}) + \tau_d = \tau + \tau_G \quad (1)$$

In "(1)", $M_{ka}(q)$ stands for the inertia matrix of the knee-ankle coupled dynamics. $V_{ka}(q,\dot{q})$ denotes the coriolis/ centripetal matrix of the system, $G_{ka}(q)$ is a vector that represents the effect of gravity, frictional terms are represented by the matrix $F_{ka}(\dot{q})$, and the disturbance torque is labeled by τ_d. Torque generated by each joint is represented by τ and τ_G is the ground reaction torque which is generated as a result of the interaction of the foot with the ground. The control input to the system is $\tau + \tau_G = [\tau_k + \tau_{G(k)} \quad \tau_a + \tau_{G(a)}] \in \mathbb{R}^2$. Here, subscript 'k' stands for knee joint and subscript 'a' stands for ankle joint. Detailed description of the terms in "(1)" are given in (Kibria & Commuri, 2024). A block diagram of the proposed neural network control system is shown in Figure 1(e).

2.3 Parameterization of the Gait Profiles and Ground Reaction Torque

Nominal displacement profiles for knee and ankle joints during gait are generated according to "(2)", where the subscript 'i' refers to either knee or ankle joint:

$$q^g_{r(i)}(t) = a^{g0}_{(i)} + \sum_{k_g=1}^{5} \{a^g_{(i)} \cos(k_g \omega^g_{(i)} t) + b^g_{(i)} \sin(k_g \omega^g_{(i)} t)\}; \quad (2)$$

Here, displacement profile time instance is represented by 't'. We can obtain the parameters $a^{g0}_{(i)}$, $a^g_{(i)}$, $b^g_{(i)}$, $\omega^g_{(i)}$ through the synthesis of the Fourier series. As the hip is under biological control, gait based desired trajectory for 'knee' and 'ankle' can be generated from hip joint movement and used as kinematic reference as following:

$$\underline{q}^g_{r(i)} = [q^g_{r(i)} \quad \dot{q}^g_{r(i)} \quad \ddot{q}^g_{r(i)}]; \quad q^g_{r(i)} = [q^g_{kr} \quad q^g_{ar}]^T;$$

$$\dot{q}^g_{r(i)} = [\dot{q}^g_{kr} \quad \dot{q}^g_{ar}]^T; \ddot{q}^g_{r(i)} = [\ddot{q}^g_{kr} \quad \ddot{q}^g_{ar}]^T; \quad (3)$$

The gait-based profiles are labeled with superscript $(\cdot)^g$ and are generated by determining the user's intent during the gait cycle. To compute the control input $\tau + \tau_G$, the ideal kinematic profiles of knee-ankle joints $\underline{q}_{r(i)} = [q^T_{r(i)} \quad \dot{q}^T_{r(i)} \quad \ddot{q}^T_{r(i)}]^T$ are not available.

The differences between the ideal kinematic references and the gait-based references are defined as:

$$\underline{\tilde{q}}^g_{r(i)} = [\tilde{q}^T_{r(i)} \quad \dot{\tilde{q}}^T_{r(i)} \quad \ddot{\tilde{q}}^T_{r(i)}]^T; \tilde{q}_{r(i)} = q_{r(i)} - q^g_{r(i)};$$

$$\dot{\tilde{q}}_{r(i)} = \dot{q}_{r(i)} - \dot{q}^g_{r(i)}; \quad \ddot{\tilde{q}}_{r(i)} = \ddot{q}_{r(i)} - \ddot{q}^g_{r(i)}; \quad (4)$$

In practice, accurate evaluation of ground reaction torque τ_G is not feasible. Therefore, gait-based ground reaction torques τ^g_G acting on knee and ankle joints are estimated from known empirical models.

The estimation errors between estimated GRT τ^g_G and actual $\tau_{G(i)}$ at the knee or ankle joints are defined as:

$$\tilde{\tau}_{G(i)} = \tau_{G(i)} - \tau^g_{G(i)}; \quad (5)$$

The actual ground reaction torque $\tau_{G(i)}$ at knee or ankle joint can be approximated by following equation (Mai & Commuri, 2016):

$$\tau^g_{G(i)}(t) = d_{z(i)} F_{x(i)}(t) + d_{x(i)} F_{z(i)}(t); \quad (6)$$

in which 't' is the gait time, $F_{z(i)}$ indicates the vertical ground reaction force and $F_{x(i)}$ is the horizontal ground reaction forces acting on the knee or ankle joints. $d_{x(i)}$ means the distances between knee joint or ankle joint to the center of pressure (ground contact point) during gait. The ground reaction forces can be computed from a nonlinear spring-damper system equations mentioned in (Peasgood et al., 2006):

$$F_{z(i)} = \bar{\kappa}(z_P)^e + c_m \dot{z}_p$$
$$F_{x(i)} = \mu F_z \, sgn(\dot{x}_h); \quad (7)$$

in which, z_P and $\dot{z}_p$ mean foot penetration and penetration rate at the ground contact point. $\bar{\kappa}$, e, c_m, μ, $sgn(\cdot)$, $\dot{x}_h$ denote respectively- spring coefficient, spring exponent, damping coefficient, friction coefficient, signum function, and the horizontal velocity.

Remark 1. In "(2)", the sine and cosine functions are bounded; it is it is assumed that the reference kinematic pattern and the gait based kinematic pattern $q^g_{r(i)}$ are also bounded as the residual limb is under active control of the user to follow specific periodic gait profile to reduce the energy consumption during a walk (Ackermann & Bogert, 2010). Hence, we can assume that $\tilde{q}_{r(i)}$ term is also bounded as it is the difference between two bounded terms.

Remark 2. In "(7)", the ground is assumed to be firm and therefore present finite penetration of the foot. Therefore, the terms $F_{z(i)}$ and $F_{x(i)}$ terms in equation (7) are bounded and gait based $\tau^g_{G(i)}$ in (5) is also bounded. Since weight of the individual is known, the actual ground reaction torque $\tau_{G(i)}$ is also bounded. Therefore, $\tilde{\tau}_{G(i)} = \tau_{G(i)} - \tau^g_{G(i)}$ is also bounded.

2.4 Cost Function for Single Support Time

To evaluate the performance of the controller in terms of single support time, a cost function is defined as:

$$J_{sp}(t) = \frac{1}{2}[e_{ft}(t_{LR})]^2 + \frac{1}{2}[e_{ft}(t_{TS})]^2 \quad (8)$$

Here, $e_{ft}(t_{LR})$ and $e_{ft}(t_{TS})$ are the foot angle error of the prosthetic leg from desired foot angle at 'Loading Response' and 'Terminal Stance' phases. Time lapse between these phases of the gait is considered as the single support time t_{SS}.

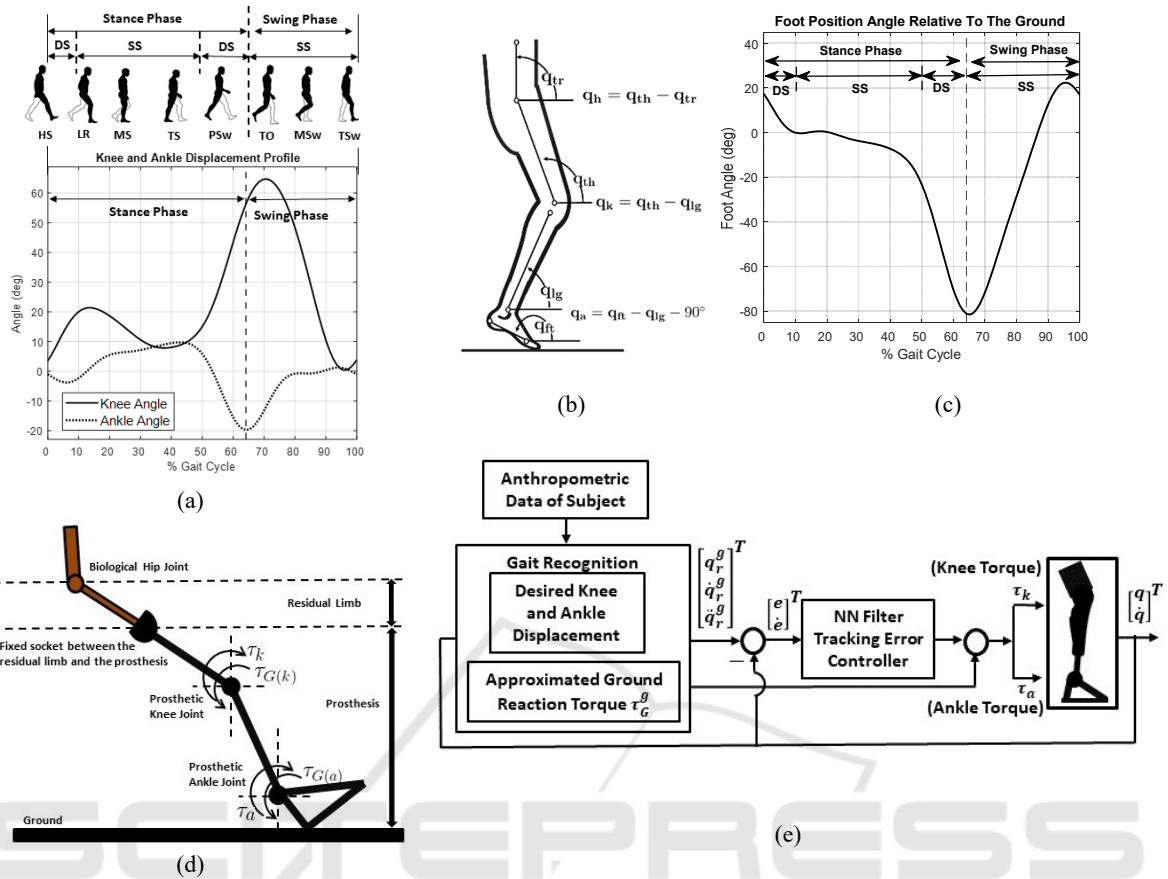$$t_{SS} = t_{TS} - t_{LR} \quad (9)$$

Figure 1: (a) Reference gait profiles of knee and ankle joints; HS = Heel Strike, LR = Loading Response, MS = Mid Stance, TS = Terminal Stance, PSw = Pre-Swing, TO = Toe Off, MSW = Mid Swing, TSw = Terminal Swing. DS = Double Support, SS = Single Support.
(b) Angle calculation for leg joints during a gait. q_{tr} = trunk angle, q_h = hip angle, q_{th} = thigh angle, q_{lg} = shank angle, q_k = knee angle, q_a = ankle angle, q_{ft} = foot angle. q_h and q_k are +ve for Flexion and -ve for Extension, q_a is +ve for Dorsiflexion and -ve for Planter Flexion.
(c) Foot angle relative to the ground. DS = Dual Support, SS = Single Support.
(d) Link-segment representation of the prosthetic leg connected to the residual limb.
(e) Block diagram of NN controlled knee-ankle Prosthetic.

in which t_{TS} and t_{LR} are the time instances of the prosthetic leg at 'Loading Response' and 'Terminal Stance' phases. If we can minimize e_{ft} at these time instances then it will in turn reduce the single support time error of the prosthetic leg, thereby reducing gait asymmetry. Since the cost function J_{sp} is a function of e_{ft}, so minimizing the cost function will result in reducing gait asymmetry.

Using Figure 1(b) the augmented cost function can be written as:

$$J_{sp}(t) = \frac{1}{2}\left[e_a(t_{LR}) - e_k(t_{LR})\right]^2 + \frac{1}{2}\left[e_a(t_{TS}) - e_k(t_{TS})\right]^2 \tag{10}$$

2.5 Control Equations

In order for the prosthetic system to ensure near natural gait cost function J_{sp} needs to be small. From (14), we see that $J_{sp} = fcn(e_k, e_a)$. So, if the controller can reduce the knee and ankle angle error then in tern it will reduce J_{sp}. To make the prosthetic system follow a reference trajectory $q_{r(i)}^g$, at first the tracking error 'e(t)' and the filtered tracking error 'r(t)' is defined by (Lewis et al., 1997):

$$e = q_{r(i)}^g - q; \quad r = \dot{e} + \lambda e \tag{11}$$

in which, λ is a positive constant, $q_{r(i)}^g = \begin{bmatrix} q_{kr}^g & q_{ar}^g \end{bmatrix}^T$; and $q = \begin{bmatrix} q_k & q_a \end{bmatrix}^T$; The dynamics of

the prosthesis in "(1)" can be expressed with reference to the filtered tracking error as:

$$M_{ka}\dot{r} = M_{ka}(\ddot{q}_{r(i)}^g - \ddot{q} + \lambda\dot{e})$$
$$= -V_{ka}r + f + \tau_d - \tau - \tau_G \quad (12)$$

Where, $f = M_{ka}(\ddot{q}_{r(i)}^g + \lambda\dot{e}) + V_{ka}(\dot{q}_{r(i)}^g + \lambda e) + G_{ka}(q) + F_{ka}(q)$.

The term f comprises of the unknown nonlinear terms in the dynamics of the system. In the next sections, we will demonstrate the use of RBF neural network to approximate f and implement a stable controller.

2.6 Neural Network (NN) Based Approximation

The function f in equation (16) is a smooth function of the joint angles and joint velocities and can be bounded on a compact region in $\mathbb{R}^2$. Hence f can be approximated using a RBF network (Schilling et al., 2001).

The output of the RBF network can be expressed as:

$$h_j = exp^{-\frac{\|x - \mu_i\|}{b_j}}; j = 1,2,3,..k \quad (13)$$
$$f(x) = \underline{W}^T h + \varepsilon$$

in which, x is the input of the network, i is input number of the network, j is the number of hidden layer nodes in the network, μ_i value represents the center point of the Gaussian function of the neural net k for the ith input, b_j is the width of the Gaussian function for neural network k. Here, $\underline{W}$ represents optimum weight for the NN and ε is a very small value. For an estimated value of $\underline{W}$, i.e. $\hat{W}$, the output of the NN is expressed as $\hat{W}^T$h(x). Learning algorithms are designed such that $\hat{W}$ is updated iteratively to minimize the error between f(x) and its estimation $\hat{f}(x)$.

$$\hat{f}(x) = \hat{W}^T h(x) \quad (14)$$

Here, $\widetilde{W} = \underline{W} - \hat{W}$; $\|\underline{W}\|_F \leq W_b$; so, $\dot{\widetilde{W}} = -\dot{\hat{W}}$;

$$f - \hat{f} = \tilde{f} = \underline{W}^T h + \varepsilon - \hat{W}^T h = \widetilde{W}^T h + \varepsilon \quad (15)$$

From the f(x) expression in equation (16) the input of the RBF has been selected as:

$x = [e_k \ \dot{e}_k \ e_a \ \dot{e}_a \ q_{kr}^g \ \dot{q}_{kr}^g \ \ddot{q}_{kr}^g \ q_{ar}^g \ \dot{q}_{ar}^g \ \ddot{q}_{ar}^g]$;
here, subscript k= knee, a=ankle, r = reference; superscripts g = gait based.

2.7 Analysis of Controlled Prosthetic Gait

The control law for the system described in "(1)" is:

$$\tau = \hat{f}(x) + K_v r - \upsilon - \tau_G^g \quad (16)$$

In which, $\hat{f}$ is the estimation of f, $\upsilon = -(\varepsilon_N + b_d)sgn(r)$ is the robust term, and τ_G^g is the gait-based ground reaction torque. The corresponding neural network adaptive law is designed as:

$$\dot{\hat{W}} = Fhr^T - \kappa F\|r\|\hat{W} \quad (17)$$

Where, κ, $F = F^T \geq 0$ are design parameters. In "(21)" the third term is the filtering term which gives a better tracking response for non-zero initial condition.

Theorem II.1. The prosthetic system given in "(12)" with the control law in "(16)" and the weight update law for the NN in "(17)" ensure that J_{sp} is bounded and the error between the desired and actual support time can be made arbitrarily small. Further, the tracking error e(t) is bounded and can be made arbitrarily small.

Proof.
Substituting "(16)" to "(12)" we can find:

$$M_{ka}\dot{r} = -(K_v + V_{ka})r + \widetilde{W}^T h + \varepsilon + \tau_d - \tilde{\tau}_G + \upsilon \quad (18)$$

Where, $\tilde{\tau}_G$ is the difference between actual and gait-based ground reaction torque.
First, the Lyapunov function is defined as:

$$L = \frac{1}{2}r^T M_{ka}r + \frac{1}{2}tr(\widetilde{W}^T F^{-1}\widetilde{W}) \quad (19)$$

Taking derivative of "(19)" we can find:

$$\dot{L} = r^T M_{ka}\dot{r} + \frac{1}{2}r^T \dot{M}_{ka}r + tr(\widetilde{W}^T F^{-1}\dot{\widetilde{W}}), \quad (20)$$

Inserting "(14)", "(18)" into "(20)", and with the help of "(15)", and "(17)" we can write:

$$\dot{L} = -r^T K_v r + \kappa\|r\|tr\{\widetilde{W}^T(\underline{W} - \widetilde{W})\} + r^T(\tau_d - \tilde{\tau}_G + \upsilon + \varepsilon) \leq -K_v\|r\|^2 + \kappa\|r\|\|\widetilde{W}\|_F(W_B - \|\widetilde{W}\|_F) + (\varepsilon_N + b_d)\|r\| \quad (21)$$

$$= -\|r\|\{K_{vmin}\|r\| + \kappa\|\widetilde{W}\|_F(\|\widetilde{W}\|_F - W_B) - (\varepsilon_N + b_d)\}$$

By setting up boundary for $\|r\|$ and $\|\widetilde{W}\|_F$ as:

$$\|r\| > \frac{\frac{\kappa}{4}W_b^2 + (\varepsilon_N + b_d)}{K_{vmin}} = \frac{B_1}{K_{vmin}} = B_r$$

$$\|\widetilde{W}\|_F > \frac{W_b}{2} + \sqrt{\frac{1}{4}W_b^2 + \frac{(\varepsilon_N + b_d)}{\kappa}} = B_w \qquad (22)$$

We can observe that in "(21)", $\dot{L}$ is negative because the term inside the braces can be written as:

$$\{K_{vmin}\|r\| + \kappa\|\widetilde{W}\|_F(\|\widetilde{W}\|_F - W_B) - (\varepsilon_N + b_d)\}$$

$$= \kappa(\|\widetilde{W}\|_F - \frac{1}{2}W_B)^2 - \frac{\kappa}{4}W_b^2 + K_{vmin}\|r\| - (\varepsilon_N + b_d)\} \qquad (23)$$

The first and fourth terms on the right side of "(23)" are positive and other terms are negative. The boundary conditions of "(22)" ensure that the derivative of the Lyapunov equation "(21)" is negative on the region described in "(22)" and implies system stability. The boundary conditions of "(22)" ensure the filtered tracking error and the error in estimated NN weights converge exponentially to the bounds expressed in "(22)". Now, from "(15)" and "(22)", we can set the bounds for error terms as:

$$\tau = \hat{f}(x) + K_v r - \upsilon - \tau_G^g \qquad (24)$$

$$\|e\| < \frac{\|r\|}{\lambda_{min}} < \frac{B_1}{\lambda_{min}K_{vmin}} \qquad (25)$$

Where, λ_{min} is the minimum design value for λ.

From "(14)" we see that the cost function J_{sp} depends on the difference between e_a and e_k. From "(14)" and "(25)" we can write:

$$\frac{1}{2}(e_a - e_k)^2 < \frac{1}{2}(\|e_a\| + \|e_k\|)^2$$
$$< \frac{1}{2}(\frac{2B_1}{\lambda_{min}K_{vmin}})^2 \qquad (26)$$

Which gives a bound on the cost function J_{sp} in "(14)":

$J_{sp} < (\frac{2B_1}{\lambda_{min}K_{vmin}})^2$; Therefore, it can be concluded that the cost function J_{sp} is bounded by design terms λ_{min} and K_{vmin}, and can be minimized by the choice of design values.

3 SIMULATION RESULTS

In this section, two simulation examples are considered to compare the performance of the proposed controller with a standard PD controller ($\tau^{PD} = K_v^{PD}(\lambda^{PD}e + \dot{e}) - \tau_G^g$) which is widely used for this type of systems. Gain parameters for both PD and NN controllers were chosen to provide stable and acceptable tracking performance. Lower gain values made the system unstable and deteriorated tracking performance. System parameters were chosen from (Kibria & Commuri, 2024; Zhou et al., 2016).

3.1 Monte-Carlo Simulation to Study Support Time

In this example, Monte Carlo simulation is performed to study the 'support time' achieved by the proposed controller. Support time is defined by the time difference between the 'Loading Response (LR)' and 'Terminal Stance (TS)' phases of the gait. In this example, 1000 different simulations are conducted with the walking speed, ground reaction force, measurement noise, disturbance torque being randomly selected. The error between the desired support time and the actual support time (TS and LR time error) is shown in Figure 2. It is seen that the proposed controller can achieve near-normal gait despite unknown changes in user gait, terrain conditions, or measurement noise (error in LR and TS time is 6.74 and 5.03 milliseconds (standard deviation of 0.13 and 0.29 milliseconds)). On the other hand, the performance of PD controller deteriorates in the presence of variations in desired gait, terrain conditions, and measurement noise (error in LR and TS time is 148.76 and 153.94 milliseconds (standard deviation of 0.97 and 0.58 milliseconds)).
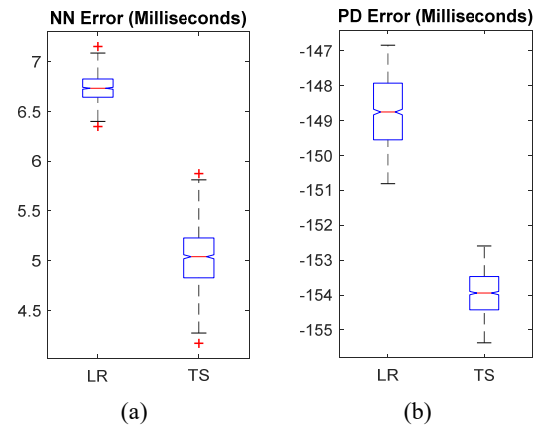

Figure 2: Monte Carlo error for NN (a) and PD (B) at Loading Response (LR), and Terminal Stance (TS) phases.

3.2 Tracking Performance

The tracking performance for nominal gait (walking at normal self-selected pace, known ground reaction force, and no disturbance torque) is considered in this example. From Figure 3, it is seen that the NN controller can track the desired knee and ankle displacement profiles with greater accuracy than the PD controller.

The simulation examples discussed in this section demonstrate that the proposed NN controller can adapt in real time to track desired joint profiles for the prosthetic leg. More importantly, the proposed controller ensures that the prosthetic foot reaches the 'Loading Response' position and maintains stipulated 'single support time' to provide near natural gait for the individual.
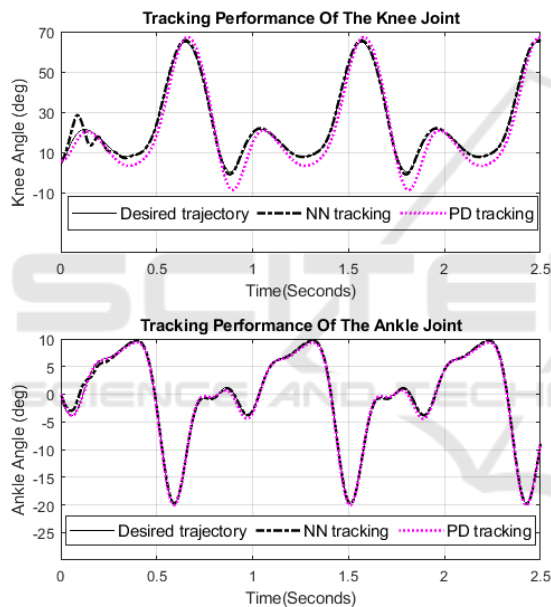

Figure 3: Gait profile tracking of knee and ankle joints.

4 CONCLUSIONS AND FUTURE WORKS

In this paper, a novel control strategy was proposed to reduce the asymmetry in gait between the intact and amputated side of an amputee. Unlike traditional controlling approach, the proposed controlling approach effectively addresses real time challenges like variations in ground reaction force, measurement noise, changes in walking speed etc., that can degrade the performance of the system. It holds great promise for prosthetics, potentially enhancing amputee

mobility, comfort, and overall quality of life. The development of a prosthetic test-bed and the validation of the control strategy discussed in this paper are being pursued by the authors.

REFERENCES

Ackermann, M., & Bogert, A. J. (2010). Optimality principles for model-based prediction of human gait. *Journal of Biomechanics*, *43*(6), 1055-1060. https://doi.org/https://doi.org/10.1016/j.jbiomech.2009.12.012

Elery, T., Rezazadeh, S., Nesler, C., & Gregg, R. D. (2020). Design and Validation of a Powered Knee–Ankle Prosthesis With High-Torque, Low-Impedance Actuators. *IEEE Transactions on Robotics*, *36*(6), 1649-1668. https://doi.org/10.1109/TRO.2020.3005533

Embry, K. R., & Gregg, R. D. (2021). Analysis of Continuously Varying Kinematics for Prosthetic Leg Control Applications. *IEEE Transactions on Neural Systems and Rehabilitation Engineering*, *29*, 232-272. https://doi.org/10.1109/TNSRE.2020.3045003

Feng, Y., & Wang, Q. (2017). Combining Push-Off Power and Nonlinear Damping Behaviors for a Lightweight Motor-Driven Transtibial Prosthesis. *IEEE/ASME Transactions on Mechatronics*, *22*(6), 2512-2523. https://doi.org/10.1109/TMECH.2017.2766205

Gao, S., Mai, J., Zhu, J., & Wang, Q. (2021). Mechanism and Controller Design of a Transfemoral Prosthesis With Electrohydraulic Knee and Motor-Driven Ankle. *IEEE/ASME Transactions on Mechatronics*, *23*(5), 2429-2439. https://doi.org/10.1109/TMECH.2020.3040369

Gorden, L. Y. T., Ariel, Y. F., Pei, H., Meng, L., Yi Zhen, N. G., & Graves, N. (2022). Decision-making for early major amputation in selected diabetic foot ulcer patients with peripheral vascular disease. *Health Care Science*, *1*(2), 58-68. https://doi.org/https://doi.org/10.1002/hcs2.17

Kibria, Z., & Commuri, S. (2024). Neuro-Dynamic Control of an Above Knee Prosthetic Leg. *SN Computer Science*, *5*(5), 509. https://doi.org/10.1007/s42979-024-02817-1

Lenzi, T., Cempini, M., Hargrove, L. J., & Kuiken, T. A. (2019). Design, Development, and Validation of a Lightweight Nonbackdrivable Robotic Ankle Prosthesis. *IEEE/ASME Transactions on Mechatronics*, *24*(2), 471-482. https://doi.org/10.1109/TMECH.2019.2892309

Lewis, F. L., Jagannathan, S., & Yeşildirek, A. (1997). Chapter 7 - Neural Network Control of Robot Arms and Nonlinear Systems. In L. E. Omid Omidvar and David (Ed.), *Neural Systems for Control* (pp. 161-211). Academic Press. https://doi.org/https://doi.org/10.1016/B978-012523430-3/50008-8

Mai, A., & Commuri, S. (2016). Intelligent control of a prosthetic ankle joint using gait recognition. *Control*

Engineering Practice, *49*, 1-13. https://doi.org/https://doi.org/10.1016/j.conengprac.2016.01.004

Pagel, A., Ranzani, R., Riener, R., & Vallery, H. (2017). Bio-Inspired Adaptive Control for Active Knee Exoprosthetics. *IEEE Transactions on Neural Systems and Rehabilitation Engineering*, *25*(12), 2355-2364. https://doi.org/10.1109/TNSRE.2017.2744987

Peasgood, M., Kubica, E., & McPhee, J. (2006). Stabilization of a Dynamic Walking Gait Simulation. *Journal of Computational and Nonlinear Dynamics*, *2*(1), 65-72. https://doi.org/10.1115/1.2389230

Saini, R. S. T., Kumar, H., & Chandramohan, S. (2020). Semi-active control of a swing phase dynamic model of transfemoral prosthetic device based on inverse dynamic model. *Journal of the Brazilian Society of Mechanical Sciences and Engineering*, *42*(6), 294. https://doi.org/10.1007/s40430-020-02387-2

Schilling, R. J., Carroll, J. J., & Al-Ajlouni, A. F. (2001). Approximation of nonlinear systems with radial basis function neural networks. *IEEE Transactions on Neural Networks*, *12*(1), 1-15. https://doi.org/10.1109/72.896792

Sharma, R., Gaur, P., Bhatt, S., & Joshi, D. (2022). Performance Assessment of Fuzzy Logic Control Approach for MR-Damper Based-Transfemoral Prosthetic Leg. *IEEE Transactions on Artificial Intelligence*, *3*(1), 53-66. https://doi.org/10.1109/TAI.2021.3106884

Winter, D. A. (2009). *Kinematics*. John Wiley and Sons Ltd. https://doi.org/https://doi.org/10.1002/9780470549148.ch3

Zhou, X., Chen, J., Chen, G., Zhao, Z., & Zhao, Y. (2016). Anthropometric body modeling based on orthogonal-view images. *International Journal of Industrial Ergonomics*, *53*, 27-36. https://doi.org/https://doi.org/10.1016/j.ergon.2015.10.007